MODELING ELECTRONEGATIVE PLASMA DISCHARGES

by

A. J. Lichtenberg, V. Vahedi, M. A. Lieberman,
and T. Rognlien

Memorandum No. UCB/ERL M93/74

15 July 1993

MODELING ELECTRONEGATIVE PLASMA DISCHARGES

by

A. J. Lichtenberg, V. Vahedi, M. A. Lieberman,
and T. Rognlien

Memorandum No. UCB/ERL M93/74

15 July 1993

ELECTRONICS RESEARCH LABORATORY

College of Engineering
University of California, Berkeley
94720

MODELING ELECTRONEGATIVE PLASMA DISCHARGES

by

A. J. Lichtenberg, V. Vahedi, M. A. Lieberman,
and T. Rognlien

Memorandum No. UCB/ERL M93/74

15 July 1993

ELECTRONICS RESEARCH LABORATORY

College of Engineering
University of California, Berkeley
94720

MODELING ELECTRONEGATIVE PLASMA DISCHARGES

by

A. J. Lichtenberg, V. Vahedi, M. A. Lieberman
Department of Electrical Engineering and Computer Sciences
and the Electronics Research Laboratory
University of California, Berkeley, CA 94720

and

T. Rognlien
Lawrence Livermore National Laboratory, Livermore, CA

Abstract

A macroscopic analytic model for a three-component electronegative plasma has been developed. Assuming the negative ions to be in Boltzmann equilibrium, a positive ion ambipolar diffusion equation is found. The electron density is nearly uniform, allowing a parabolic approximation to the plasma profile to be employed. The resulting equilibrium equations are solved analytically and matched to an electropositive edge plasma. The solutions are compared to a simulation of a parallel-plane r.f. driven oxygen plasma for two cases: (1) $p = 50$ mTorr, $n_{eo} = 2.4 \times 10^{15}$ m^{-3}, and (2) 10 mTorr, $n_{eo} = 1.0 \times 10^{16}$ m^{-3}. In the simulation, for the low power case (1), the ratio of negative ion to electron density was found to be $\alpha_0 \approx 8$, while in the higher power case $\alpha_0 \approx 1.3$. Using an electron energy distribution that approximates the simulation distribution by a two-temperature Maxwellian, the analytic values of α_0 are found to be close to, but somewhat larger, than the simulation values. The average electron temperature found self-consistently in the model is close to that in the simulation. The results indicate the need for determining a two-temperature electron distribution self-consistently within the model.

I Introduction

The equilibrium of a parallel-plane two-species low pressure plasma (positive ions and Maxwellian electrons) is well characterized by: (1) an ion diffusion equation determining the electron temperature and the plasma profile; and (2) power balance equation determining the central density in terms of the total energy absorbed by the electrons. The equilibrium analysis assumes the Bohm velocity is attained at the plasma edge with the position of the edge known [1]. This is not, of course, a complete self-consistent characterization unless the heating mechanism is also specified. Much recent work has been done in analyzing the heating mechanism in plane-parallel r.f. discharges at 13.56 MHz. At that frequency the electrons respond to the r.f. fields while the ions respond to the average fields. The heating can be obtained in terms of the r.f. current, which together with the Child Langmuir relation for the ion current in the sheath, relates these currents to sheath voltages and an average sheath thickness. The self-consistent picture was first developed for ohmic heating [2,3] and later for stochastic sheath heating, which dominates in low pressure discharges [4,5]. However, results from the self-consistent analytic models do not agree closely with experiments [1]. This is primarily because the sheath heating creates two temperature time-dependent electron energy distributions, as seen in simulations [6,7,8]. Analytic theory including these effects has brought theory and experiment much closer together [8].

No comparable analysis exists for electronegative plasmas. An ambipolar diffusion coefficient has been obtained for a three component plasma (positive ions, negative ions, and electrons) under the assumption that the electrons and negative ions are in Boltzmann equilibrium [9]. The Bohm condition at the sheath edge has also been modified to account for the presence of negative ions [10,11,12], and checked against simulation [13]. The continuity and force equations for the three species have been solved numerically to obtain the equilibrium for a positive column [14]. However, a complicated solution of this type gives little insight into the importance of various terms in the equations, and the scaling with parameters. A simpler set of equations has been used to solve qualitatively for the parameters of a negative ion source [15]. It is not straightforward to extend these analyses to a self consistent treatment, including power input and sheath formation, as has been done for two-species plasmas.

In order to make a realistic calculation of electronegative plasma equilibrium the reaction rate constants must be known. Furthermore, these rate constants must be consistent with the approximation of a three-component plasma if that approximation is to be used. There is a wealth of information on reaction rates of the various components that are generated from particular feedstock gases. For this study we consider O_2 as the feedstock gas. The rate constants for this gas [16] have been compiled for use in a simulation code [17]. The size of the rate constants and the results of simulations indicate that it is a good approximation to consider that

the equilibrium dynamics are controlled by three plasma species and the neutral gas. The important reaction-rate constants for the charged particles are

$$K_{iz} = 2.13 \cdot 10^{-14} \exp(-14.5/Te) \quad \mathrm{m^3/s} \tag{1.1}$$
$$K_{att} = 7.89 \cdot 10^{-17} \exp(-3.07/Te) \quad \mathrm{m^3/s} \tag{1.2}$$
$$K_{rec} = 1.4 \cdot 10^{-13} \quad \mathrm{m^3/sec} \tag{1.3}$$
$$K_{cx} = 3.95 \cdot 10^{-16} \quad \mathrm{m^3/sec,} \tag{1.4}$$

where K_{iz}, K_{att}, K_{rec}, K_{cx} are the rate constants for the reactions

$$O_2 + e \rightarrow O_2^+ + 2e, \quad \text{(ionization)} \tag{1.5}$$
$$O_2 + e \rightarrow O^- + O, \quad \text{(dissociative attachment)} \tag{1.6}$$
$$O_2^+ + O^- \rightarrow O_2 + O, \quad \text{(recombination)} \tag{1.7}$$
$$O_2^+ + O_2 \rightarrow O_2^+ + O_2, \quad \text{(scattering)}$$
$$O_2^+ + O_2 \rightarrow O_2 + O_2^+, \quad \text{(charge exchange)} \tag{1.8}$$
$$O^- + O_2 \rightarrow O^- + O_2. \quad \text{(scattering)} \tag{1.9}$$

The latter 3 reactions lead to effective diffusion coefficients for positive and negative ion species. The rule constant for charge transfer of O^- on O_2 is small because the threshold energy required for this process is $\sim$ 1.0 eV, which is much higher than the thermal energy of the heavy particles; hence this process is unimportant. The simulations include many other reactions, e.g. vibrational excitations, which mainly go into the calculation of the energy loss per ionization, which we will take here as a known quantity.

The goal of this paper is to develop the simplest analytical model that can predict the values of the plasma quantities such as electron and negative ion densities and electron temperature, as the neutral pressure and power to the plasma are

varied. By comparing the results against simulations the effects of the various approximations can be evaluated. In Section II we develop the basic equilibrium equations for a three-component plasma. In Section III approximate solutions are obtained for these equations. In Section IV these solutions are compared to results of simulations. In Section V the significance of the results is discussed indicating the additional information that is needed to obtain a fully self-consistent model.

II Energy and Particle Balance in Electronegative Plasmas

As in electropositive plasmas, for each charged species we can write a flux equation

$$\Gamma_i = -D_i \nabla n_i + n_i \mu_i E_i \tag{2.1}$$

where $D_i = kT_i/m_i\nu_i$, $\mu_i = |q_i|/m_i\nu_i$, with ν_i the total momentum transfer collision frequency. In equilibrium the sum of the currents must balance:

$$\sum_{i=1}^{n} q_i \Gamma_i = 0, \tag{2.2}$$

where the summation is over the n charged species. From charge neutrality we also have

$$\sum_{i=1}^{n} q_i n_i = 0, \tag{2.3}$$

which is the usual plasma approximation.

To make the algebra relatively simple we consider an oxygen plasma in which only three species need be considered: O_2^+, created by electron impact ionization, O^-, created by dissociative attachment, and electrons. All species are singly

charged, so that (2.2) becomes

$$\Gamma_+ = \Gamma_- + \Gamma_e, \tag{2.4}$$

(2.3) becomes

$$n_+ = n_- + n_e, \tag{2.5}$$

and the equations of (2.1) are

$$\begin{aligned} \Gamma_+ &= -D_+ \nabla n_+ + n_+ \mu_+ E, \\ \Gamma_- &= -D_- \nabla n_- - n_- \mu_- E, \\ \Gamma_e &= -D_e \nabla n_e - n_e \mu_e E. \end{aligned} \tag{2.6}$$

Using these five equations we can eliminate Γ_-, Γ_e, n_+, n_e, and E to obtain an equation in Γ_+, $\alpha = n_-/n_e$, and the gradients

$$\Gamma_+ = -\frac{(\mu_e + \mu_- \alpha) D_+ + \mu_+ (1+\alpha) D_e \dfrac{\nabla n_e}{\nabla n_+} + \mu_+ (1+\alpha) D_- \dfrac{\nabla n_-}{\nabla n_+}}{\mu_e + \mu_- \alpha + \mu_+ (1+\alpha)} \nabla n_+. \tag{2.7}$$

We have factored out ∇n_+ to put the equation formally in the usual form of an ambipolar diffusion coefficient

$$\Gamma_+ = -D_{+a} \nabla n_+, \tag{2.8}$$

but we note that this is not equivalent to D_a for electropositive plasmas as D_{+a} is a function of position both through α and through the gradients.

The form (2.7) was derived by Rogoff [18] and also, implicitly, by Thompson [9]. However, because (2.8) depends explicitly on the other variables it cannot be

independently solved for n_+, but is coupled to n_- and n_e. In this form three diffusion equations must be written for the three variables, and solved simultaneously. This is clearly a difficult numerical procedure. Thompson [9] attempted to circumvent this difficulty by assuming that both negative species are in Boltzmann equilibrium and thus the logarithmic gradients are related by their temperature ratio. Although this assumption is valid for the mobile electrons, it is not necessarily valid for the negative ions. With this caveat, we introduce the temperature ratio

$$\gamma = T_e/T_i, \tag{2.9}$$

where T_i is the temperature of both ionic species; typically $\gamma \sim 100 \gg 1$. Then the Boltzmann relation applied to each species yields

$$\frac{\nabla n_-}{n_-} = \gamma \frac{\nabla n_e}{n_e}. \tag{2.10}$$

Using (2.10) together with

$$\nabla n_+ = \nabla n_- + \nabla n_e,$$

we obtain the ratios

$$\frac{\nabla n_e}{\nabla n_+} = \frac{1}{1+\gamma\alpha}, \quad \frac{\nabla n_-}{\nabla n_+} = \frac{\gamma\alpha}{1+\gamma\alpha}. \tag{2.11}$$

Substituting (2.11), together with the Einstein relations

$$\frac{D_-}{D_+} = \frac{\mu_-}{\mu_+} \quad , \quad \frac{D_e}{D_+} = \gamma \frac{\mu_e}{\mu_+},$$

into (2.7), then we obtain, after a little algebra,

$$D_{a+} = D_+ \frac{(1+\gamma+2\gamma\alpha)\left(1+\alpha\frac{\mu_-}{\mu_e}\right)}{(1+\gamma\alpha)\left(1+\frac{\mu_+}{\mu_e}(1+\alpha)+\frac{\mu_-}{\mu_e}\right)}, \tag{2.12}$$

which is the form given by Thompson. We note immediately, since μ_-/μ_e, $\mu_+/\mu_e \ll 1$, that for all reasonable cases the second parenthesis in both the numerator and denominator are approximately equal to one, yielding

$$D_{a+} \cong D_+ \frac{1+\gamma+2\gamma\alpha}{1+\gamma\alpha}. \tag{2.13}$$

Thompson [9] plotted D_{a+} from (2.12) with α as a parameter. The structure is easily seen from the simpler form (2.13). For $\alpha \gg 1$, γ cancels such that $D_{a+} \cong 2D_+$. When α decreases below 1, but $\gamma\alpha \gg 1$, $D_{a+} \cong D_+/\alpha$ such that D_{a+} increases inversely with decreasing α. For $\gamma\alpha < 1$, $D_{a+} \cong \gamma D_+$, which is the usual ambipolar diffusion without negative ions. For plasmas in which $\alpha \gg 1$ is initially the entire transition region takes place over a small range of $1/\gamma < \alpha < 1$, such that the simpler value of $D_{a+} = 2D_+$ holds over most of the plasma, except near $n_- \approx 0$.

Consider now the positive ion diffusion equation, keeping only the dominant reaction rate constants. For simplicity we also restrict our attention to the one-dimensional plane-parallel geometry. We have

$$-\frac{d}{dx}\left(D_{a+}(\alpha)\frac{dn_+}{dx}\right) = K_{iz}n_0n_e - K_{rec}n_+n_-, \tag{2.14}$$

where n_0 is the neutral gas density. Equation (2.14) can not be solved directly, as it is a function of n_- and n_e (through α) as well as n_+. However, we can integrate (2.10) to obtain

$$\frac{n_e}{n_{e0}} = \left(\frac{n_-}{n_{-0}}\right)^{1/\gamma}, \tag{2.15}$$

from which we can eliminate n_e. We can then use charge neutrality (2.5) to eliminate n_-, such that (2.14) becomes

$$-\frac{d}{dx}\left(D_{a+}(n_+)\frac{dn_+}{dx}\right) = K_{iz}n_0n_e(n_+) - K_{rec}n_+n_-(n_+) \tag{2.16}$$

where $D_{a+}(n_+)$ is a rather complicated function of n_+ and one arbitrary constant $\alpha_0 = n_{-0}/n_{e0}$, the ratio of n_- to n_e at the plasma center. It is now possible to integrate (2.16) numerically, given the arbitrary constants. From (2.15) we can set $n_e \cong n_{e0}$ in (2.16).

In electropositive plasma we have two constants n_{e0} and T_e. We now have an additional constant, α_0. We therefore need three relations rather than the two, power balance and particle balance for positive ions, required for electropositive plasmas. A relation that we have not yet used is the particle balance of negative ions. Assuming the negative ion flux goes to zero at the sheath edge, we then have the equations: positive ion particle balance,

$$-D_{a+}\frac{dn_+}{dx}\bigg|_{x=\ell} = \int_0^\ell K_{iz}n_0n_e dx - \int_0^\ell K_{rec}n_+n_-(n_+)dx; \tag{2.17}$$

negative ion particle balance,

$$\int_0^\ell K_{att} n_0 n_e dx - \int_0^\ell K_{rec} n_+ n_-(n_+) dx = 0; \tag{2.18}$$

and energy balance for the electrons,

$$P_{abs} = 2\mathcal{E}_c \int_0^\ell K_{iz} n_0 n_e dx; \tag{2.19}$$

where $\mathcal{E}_c(T_e)$ the electron energy lost per electron-positive ion pair created, is a known function of T_e. Given the plasma length 2ℓ, and power P_{abs}, the three equations can be simultaneously solved for the three unknowns T_e, α_0, and n_{+0}. However, the plasma edge ℓ is not exactly known, but is dependent on the Bohm flux condition [10–13]

$$-D_{a+} \frac{dn_+}{dx}\bigg|_{x=\ell} = n_+(\ell) u_B(T_e, T_i, \alpha), \tag{2.20}$$

which indicates where the sheath begins. The Bohm velocity in (2.20) has a more general form than the usual expression $u_B = (eT_e/M_+)^{1/2}$ [10, 13] since negative ions may be present when (2.20) is satisfied.

The more general form is

$$u_B = \left[\frac{eT_e(1+\alpha)}{M(1+\gamma\alpha)}\right] \tag{2.21}$$

For $\alpha > 1/\gamma$, the negative ions significantly reduce the Bohm velocity.

There are actually three different electronegative discharge equilibrium regimes depending on neutral pressure and applied power. (1) At low pressure and high

power, α_0 is small. The negative ion density becomes quite small well within the plasma volume, such that much of the edge region behaves essentially electropositively. (2) In the opposite limit of high pressure and low power, $\alpha_0 \gg 1$ and a significant density of negative ions may exist where (2.20) is satisfied, giving a significantly depressed Bohm velocity. (3) We might expect a large intermediate region to exist where the central α may be quite large but the edge α is near zero, allowing the usual Bohm velocity to be used. We examine this further in the following section, where we compare the solutions of (2.17)–(2.20) to plasma simulations. We find that there is usually a significant edge region in which the plasma is essentially electropositive.

If α_0 is large, then $D_{a+} = 2D_+$ over most of the plasma. We might then ask whether a simpler solution with $D_{a+} = 2D_+$ and $n_e = n_{e0}$ might be adequate to describe the bulk plasma. Numerical calculations (see next section) indicate that this is reasonable. However, there is not much to gain over solving the more complete equations, as the nonlinearity in the third term of (2.16) does not permit an analytical solution for n_+ to be given explicitly.

III Approximate Solutions

Equations (2.17)–(2.20) are difficult to solve simultaneously. In this section we make the necessary assumptions to obtain approximate analytic solutions. The justification will be the comparison with simulations in the following section.

Consider the simpler problem in which α is sufficiently large that $D_{a+} \cong 2D_+$, but the effect of recombination can be neglected in determining the spatial distribution. The diffusion equation (2.16) then takes the simple form

$$2D_+ \frac{d^2 n_+}{dx^2} = K_{iz} n_0 n_{e0}, \tag{3.1}$$

where (2.15) allows us to set $n_e \cong n_{e0}$. In this approximation $n_+(x)$ has a simple parabolic solution of the form

$$\frac{n_+}{n_{e0}} = \alpha_0 \left(1 - \frac{x^2}{\ell^2}\right) + 1, \tag{3.2}$$

where ℓ is the nominal position where $\alpha = 0$. We would not normally expect the Bohm flux condition to be met within the validity of this solution, so the $\alpha \gg 1$ solution must be matched to an $\alpha = 0$ electropositive solution which in turn determines the position of the plasma edge satisfying (2.20).

We further simplify our analysis by assuming that n_{e0} is known. The absorbed power P_{abs} is then obtained *a posteriori* from (2.19). If P_{abs} is specified rather than n_{e0}, then n_{e0} can be obtained iteratively, as is done for temperature, as described below.

Substituting (3.2) in (2.17) and (2.18) and integrating, we obtain, respectively,

$$K_{iz} n_0 \ell = K_{rec} n_{e0} \left(\frac{8}{15}\alpha_0^2 + \frac{2}{3}\alpha_0\right) \ell + \frac{4D_+ \alpha_0}{\ell}, \tag{3.3}$$

$$K_{att} n_0 = K_{rec} n_{e0} \left(\frac{8}{15}\alpha_0^2 + \frac{2}{3}\alpha_0\right), \tag{3.4}$$

where the integration is only over the strongly electronegative plasma. At $x = \ell$ this electronegative solution is matched to the usual electropositive solution [1]

$$n_+ = n_e = \bar{n}\cos[\kappa(x - x_0)]$$

where $\kappa = (\nu_{iz}/D_a)^{1/2}$ with $\nu_{iz} = K_{iz}n_0$ and $D_a \cong \gamma D_+$, from (2.13). The matching conditions, at $x = \ell$, for density and ion flux are

$$\bar{n}\cos[\kappa(\ell - x_0)] = n_{e0} \tag{3.5}$$

and

$$D_a\kappa\bar{n}\sin(\ell - x_0) = \frac{4D_+\alpha_0 n_{e0}}{\ell} \tag{3.6}$$

The Bohm flux condition in the electropositive region is

$$D_a\kappa\sin[\kappa(\ell_p - x_0)] = \cos[\kappa(\ell_p - x_0)]u_B(T_e) \tag{3.7}$$

where ℓ_p is the nominal plasma edge. Equations (3.3)–(3.7) are five relations for the five unknowns T_e, α_0, ℓ, $\bar{n}$, and x_0.

Although the above set can be readily solved numerically, further insight into the form and scaling of the solution can be obtained from an additional approximation to obtain an algebraic form. We approximate the electropositive region with a parabolic solution

$$n = n_2\left(1 - \frac{x^2}{\ell_2^2}\right), \tag{3.8}$$

such that the matching condition between the electronegative and electropositive regions, (3.5) and (3.6), are simplified to

$$n_2\left(1-\frac{\ell^2}{\ell_2^2}\right)=n_{e0} \tag{3.9}$$

and

$$2D_a n_2 \ell/\ell_2^2 = 4D_+\alpha_0 n_{e0}/\ell. \tag{3.10}$$

The Bohm flux condition (3.7) simplifies to

$$2D_a\ell_p/\ell_2^2=\left(1-\frac{\ell_p^2}{\ell_2^2}\right)u_B. \tag{3.11}$$

We can now eliminate the intermediate variables n_2 and ℓ_2 from (3.9) and (3.10) and use the Bohm flux condition to solve for ℓ:

$$\ell^2=\frac{2D_+\alpha_0}{D_a+2D_+\alpha_0}\left(\frac{2D_a\ell_p}{u_B}+\ell_p^2\right). \tag{3.12}$$

Equation (3.12) can now be used, together with (3.3) and (3.4) to obtain the three variables of our problem α_0, T_e, and ℓ.

The above equations are solved readily by noting that K_{iz} is a strong exponential function of T_e, such that the temperature is essentially clamped by the particle balance of positive ions. We can therefore take the temperature as given from (3.3) and solve for α_0 in (3.4). With this value of α_0, ℓ is obtained from (3.12) and a new temperature obtained from (3.3) after substituting the initial values of α_0 and ℓ. In

this way the complete solution is obtained by iteration. The important scaling is obtained from (3.4). Solving for α_0 we obtain

$$\alpha_0 = -\frac{5}{8} + \sqrt{\left(\frac{5}{8}\right)^2 + \frac{15}{8}\frac{K_{att}}{K_{rec}}\frac{n_0}{n_{e0}}}. \tag{3.13a}$$

For large α_0 this reduces to

$$\alpha_0 \cong \left(\frac{15}{8}\frac{K_{att}}{K_{rec}}\frac{n_0}{n_{e0}}\right)^{1/2}. \tag{3.13b}$$

Taking $n_{-0} \simeq n_{+0}$, we substitute $n_{e0} \simeq n_{+0}/\alpha_0$ into (3.13b), and solving for α_0 yields

$$\alpha_0 \simeq \frac{15}{8}\frac{K_{att}}{K_{rec}}\frac{n_0}{n_{+0}}. \tag{3.13c}$$

From (3.13c) we see the essential scaling of α_0, which increases as n_0 with increasing pressure, and decreases with increasing power. The exact scaling with power depends on whether the surface losses are large or small compared to the volume losses. Using (2.19) we rewrite (2.17) as

$$P_{abs} = -\mathcal{E}_c D_{at}\frac{dn_+}{dx}\bigg|_{x=\ell} + \int_0^\ell K_{rec} n_+ n_- dx. \tag{3.14}$$

Considering all temperature dependences as weak, and taking $n_{-0} \simeq n_{=0}$, as previously, we see that the scaling of n_{+0} with P_{abs} varies from $n_{+0} \propto P_{abs}$ (surface losses dominating) which determines the scaling of α_0 with power in (3.13c).

Before turning to a comparison of the analytic model with simulations, we note an additional complication that is important for low pressure capacitively coupled r.f. discharges, which may also be present in other types of discharges. In both

experiments and simulations the electron distribution is found to be non-Maxwellian with higher temperature tails [8]. Because of the strong exponential dependence of the ionization cross sections, the higher temperature tails may dominate the positive ion particle balance, while only having a modest effect on the negative ion balance. Assuming this situation to hold, which we shall justify in the next section, we separate the electron distribution into a two-component Maxwellian. The normalized densities of the two components are written as $\alpha_{eh} = n_{eh}/n_e$ and $\alpha_{ew} = n_{ew}/n_e$ with n_{eh} and n_{ew} being the hot tail and warm bulk components, both taken as Maxwellian. The electron temperature dependent reactions are designated as K_{atth}, K_{attw}, K_{izh}, and K_{izw}. In terms of these new variables and coefficients, (3.3) and (3.4) are rewritten

$$(K_{izh}\alpha_{eh} + K_{izw}\alpha_{ew})n_0\ell = K_{rec}n_{e0}\left(\frac{8}{15}\alpha_0^2 + \frac{2}{3}\alpha_0\right)\ell + \frac{4D_+\alpha_0}{\ell} \tag{3.15}$$

and

$$(K_{atth}\alpha_{eh} + K_{attw}\alpha_{ew})n_0 = K_{rec}n_{e0}\left(\frac{8}{15}\alpha_0^2 + \frac{2}{3}\alpha_0\right). \tag{3.16}$$

Comparing the terms on the L.H.S. of (3.15) it is clear with the strong exponential temperature dependence of K_{iz} that the hot component will dominate the ionization for modest temperature separations and tail densities that are a significant fraction of the whole. For example, using K_{iz} from (1.1) and nominal values of $T_{eh} = 3\text{eV}$,

T_{ew} = 1.5eV and α_{eh}/α_{ew} = 0.25, similar to those of the simulation in the next section, we find

$$\frac{K_{izh}\alpha_{eh}}{K_{izw}\alpha_{ew}} = \frac{1}{4}\frac{\exp(-14.5/3)}{\exp(-14.5/1.5)} = 31, \tag{3.17}$$

which indicates that essentially all ionization is by the hot species. From (3.15), with α_0 large, we obtain

$$\alpha_0 = \left[\frac{15}{8}\frac{(K_{atth}\alpha_{eh} + K_{attw}\alpha_{ew})}{K_{rec}n_{e0}}n_0\right]^{1/2}. \tag{3.18}$$

Using the same values as above, we find

$$\frac{K_{atth}\alpha_{eh}}{K_{attw}\alpha_{ew}} = \frac{1}{4}\frac{\exp(-3.07/3)}{\exp(-3.07/1.5)} = 0.7, \tag{3.19}$$

i.e. the two terms are comparable. The result is that with a smaller value of α_{eh}, in the two temperature case, α_0 will also be smaller, while the positive ion balance equation will not be much changed.

IV Comparison With Simulation

We compare our analytic theory with simulation of a capacitive parallel-plate capacitive r.f. discharge in oxygen. The simulations were done with one-dimensional dynamics using a particle-in-cell code (PDP1) [17], which included the most important collisional processes using Monte Carlo methods. The principle macroscopic coefficients used in the simulation and the analytic model have been given in the introduction. The details of the simulation and the results are given elsewhere [19].

For the purpose of comparison with the analytic model, two cases with widely differing parameters have been chosen: (1) $p = 50$ mTorr ($n_0 = 1.6 \cdot 10^{21}$ m^{-3}) at low power ($n_{e0} = 2.4 \cdot 10^{15}$ m^{-3}); and (2) $p = 10$ mTorr ($n_0 = 3.2 \cdot 10^{20}$ m^{-3}) at higher power ($n_{e0} = 1.0 \cdot 10^{16}$ m^{-3}). For both cases a 13.56 MHz constant current source is used in the simulation to supply the power. The plate spacings used were 4.5 cm and 6 cm, respectively, in the two cases. As we are concerned here with the comparison of equilibrium dynamics, the plasma width to the sheath edge ($u = u_B$) will be the comparison length, rather than the plate spacing. The sheath thickness can be calculated *a posteriori* using the r.f. voltage measured in the simulation, but is not part of the present comparison.

As we are interested in the accuracy of the various components of the theory, we separately check these components, using simulation data. Our first check concerns the applicability of the basic diffusion coefficient (2.13) in the presence of significant recombination. To determine this we use the values D_{a+}, γ, α_0, found from the simulations and integrate (2.16) numerically from the plasma center. We compare the plasma profile with that found in the simulation. This is done for the high pressure, low power case, in which the effect of recombination is most important. The comparison is shown in Fig. 1, indicating good agreement between simulation and numerical integration of (2.16) in the electronegative regime, but disagreement in the electropositive edge region. The implication for the electronegative region is

that the analytical model holds reasonably well for negative ions, even in the presence of high recombination (in this case $\alpha_0 = 8$). Here the ionization is by the hot electron species, and the diffusion coefficient is determined by the ion temperature, both of which are well characterized. In the electropositive region, on the other hand, the ambipolar diffusion coefficient is determined by the lower electron temperature of the colder electron species, which gives a more rapid density variation in the simulation. The result indicates the need for a two-temperature description of the electron distribution, as described by (3.15) and (3.16), and more fully below.

A second test of the analytic theory is to see how well the approximation of a parabolic profile agrees with the simulation. This is shown in Fig. 2 (dashed curve) in the electronegative region. We find a reasonable agreement for $\alpha > 2$. For smaller α, the variation of $D_a(\alpha)$ with nearly constant flux results in a variation of dn/dx is not captured by the parabolic approximation. For large α_0 this is mainly an edge effect and should only have a minor impact on the integrated solutions. As seen below, the greater test of the approximation comes for $\alpha_0 = 2$ when $D_{a+}(\alpha)$, in (2.13) is continuously varying.

For the complete comparison of the equilibria we use the approximate analytic results derived in Section III. We approximate the electron distribution with two Maxwellian classes. For the two cases we are considering, the simulation results for the energy distributions are shown in Fig. 3 [19]. Using the first change in slope to

distinguish these distributions we can estimate ratios of temperatures and densities of the two species:

$$\frac{T_{eh}}{T_{ew}} \cong 1.9, \quad \frac{n_{ew}}{n_{eh}} \cong 3.9 \ (p = 50 \text{ mTorr}), \tag{4.1a}$$

$$\frac{T_{eh}}{T_{ew}} \cong 2.8 \quad \frac{n_{ew}}{n_{eh}} \cong 10 \ (p = 10 \text{ mTorr}). \tag{4.1b}$$

We note that this approximation is not unique, and that hotter electron distributions at much lower density could also be added. We discuss this point further in Section V.

Considering first the high pressure case. We "short circuit" the iterative procedure, by choosing a reasonable initial guess of $T_{eh} = 3$ eV. Using the two-temperature expression for α_0 in (3.18) we find $\alpha_0 = 11.1$, which is approximately 30 percent higher than the simulation value. From (3.12) we obtain $\ell = 0.69\ \ell_p$. Using (3.14) we find that $T_{eh} = 3.3$ eV, which is ten percent higher than the T_{eh} assumed. Since the values of α_0 and ℓ/ℓ_p found using $T_{eh} = 3$ eV are only weakly dependent on T_{eh}, we do not perform the iteration on T_{eh}. The average electron temperature in the simulation is found to be $T_e \cong 2$ eV, which is in reasonable agreement with $T_e = 2.05$ eV predicted by the model. The profile which we have calculated (dashed curve) is compared with the simulation in Fig. 4, showing reasonable agreement.

From (3.14), we can compare the integrated recombination flux Γ_{rec} (first term on the RHS), with the flux Γ_ℓ leaving the electronegative region (second term on the RHS). Substituting the numbers from our numerical case we find $\Gamma_{rec}/\Gamma_\ell = 0.26$.

This is apparently sufficiently small that the parabolic form (3.2) of the profile, which is exact in the limit of $\Gamma_{rec} = 0$, fits quite well.

The condition that the negative ions are in Boltzmann equilibrium is checked by comparing the particle flux for n_-

$$\Gamma_-(x) = \int_0^x K_{att} n_0 n_e dx - \int K_{rec} n_+ n_- dx, \tag{4.2}$$

with the terms on the right in the flux equation

$$\Gamma_- = -D_- \nabla n_- - n_- \mu_- E. \tag{4.3}$$

Since Boltzmann equilibrium is calculated by setting the R.H.S. of (4.3) equal to zero, the condition is that

$$|\Gamma_-| \lesssim \left| D_- \frac{dn_-}{dx} \right| \tag{4.4}$$

where Γ_- is obtained from (4.2).

For our model in the negative ion region, $n_e = n_{e0}$, n_+ is given by (3.2), $n_- = n_+ - n_{e0}$, and $K_{att}\ n_0$ in (4.1) is given by (3.4). Making these substitutions and perform the integration in (4.2) we obtain, approximately, for $\alpha \gtrsim 1$ and $x^2/\ell^2 \ll 1$

$$\Gamma_- \simeq \frac{7}{15} K_{rec} n_{e0}^2 \alpha_0^2 x \tag{4.5}$$

Substituting (4.5) in (4.4) and evaluating $\frac{dn_-}{dx}$ we obtain

$$\frac{7}{15} K_{rec} n_{e0}^2 \alpha_0^2 x \lesssim 2 n_{e0} \alpha_0 D_- \frac{-x}{\ell^2}. \tag{4.6}$$

We see that the factor $n_{e0}\alpha_0 x$ cancels in (4.6) such that the Boltzmann condition is satisfied independent of x. Substituting the numbers for our example, we find the ratio of the two terms in (4.6) to give

$$\frac{7K_{rec}n_{e0}\alpha_0}{30D_-/\ell^2} = 0.47$$

which reasonably satisfies the inequality.

We now compare the analytic solution to the simulation for the low pressure, high power case, for which α_0 is expected to be much smaller. From (4.6) we see that the Boltzmann equilibrium is well satisfied, but the approximation of constant $D_{a+} \cong 2D_+$ is seen from (2.13) to be quite poor. From (4.9b) the hot component is a much smaller fraction of the total electron density, and thus to obtain particle balance we would expect a significantly higher temperature. We take $T_{eh} \cong 4.5$ eV as a nominal first guess. Repeating the steps for the higher pressure case, from (3.13a) we find $\alpha_0 = 1.52$. From (2.13) we find

$$D_{a+}(\alpha_0) = 2.7D_+. \tag{4.10}$$

Replacing $2D_+$ with $D_{a+}(\alpha_0)$ in (3.12) and taking $\ell_p = 1.8$ cm and $T_{ew} \cong 1.5$ eV we find $\ell/\ell_p = 0.31$. From (3.14) we obtain $T_{eh} = 4.9$ eV, which is again approximately 10 percent higher than the assumed T_{eh}, and within the accuracy of the calculation; hence we do not iterate. The analytic and simulation profiles for n_- are compared in Fig. 5. The difference in shape is accounted for by the continuous variation of D_{a+}, as α decreases.

The results from two-component theory can be used at the plasma edge to determine all plasma parameters in terms of P, ℓ, and a single electrical parameter in a capacitive r.f. discharge. Assuming that the r.f. driving voltage is the parameter, we can obtain the sheath thickness from a modified Child-Langmuir law for r.f. driven plasmas [5]

$$J_{ion} \simeq \frac{5}{6}\left(\frac{2e}{M}\right)^{1/2} \epsilon_0 \frac{V_{rf}^{3/2}}{s_0^2} = en_s u_B \tag{4.11}$$

where we have equated the ion flux in the sheath to the Bohm flux. We have substituted $V_{dc} \cong V_{rf}$ which is the approximate condition for average electron and positive ion flux to be equal at the sheath edge. From (4.11) with V_{rf} known we can calculate the sheath width s_0. Taking $V_{rf} = 222$ volts from the simulation, and calculating $n_s = 0.26 n_{e0}$ from (3.9) and (3.11), we obtain $s_0 = 1.1$ cm. Comparing this result to the distance between the sheath edge $u_i = u_B$ and the electrode surface in Fig. 4 we find good agreement. To compute the power lost by the electrons from (2.19), we must know $\mathcal{E}_c(T_e)$, which depends on a complicated integration of a large number of rate constants for different processes over the distribution [17]. the power lost by the ions is calculated from

$$P_i \simeq en_s u_B V_{rf}. \tag{4.12}$$

We do not do these numerical calculations here.

In order to determine all plasma quantities in terms of V_{rf}, p, and ℓ we must have one additional relation between n_{e0} and V_{rf}. Such a relationship involves the

heating mechanisms [4,5] and has been used in obtaining analytic solutions to two component plasmas [1,8]. These calculations involve considerable complications and only give approximate values of n_{e0}. We do not perform the calculation here.

V Conclusion and Discussion

We have developed the macroscopic equations that are required for determining the equilibrium of an electronegative plasma, based on the Thompson [9] form of the electronegative ambipolar diffusion coefficient which assumes that the negative ions are in Boltzmann equilibrium with the fields. The approximations that are necessary to obtain the model have been examined by comparison with a particle-in-cell simulation of an oxygen plasma in a plane-parallel configuration. It was found that, over a wide range of parameters, the model is in agreement with the simulations, even though the negative ions are not in Boltzmann equilibrium with the internal electric fields. The model results in an electron density that is essentially clamped to a constant value in all but a thin edge region. For this situation, and for strongly electronegative plasmas, a parabolic approximation to the density profile can be made, leading to a simplified set of equations that can be treated fully analytically.

Over a wide range of parameters, the flux at the edge of the electronegative region, $\alpha \equiv n_-/n_e \ll 1$, is well below the modified Bohm flux, requiring the matching of the electronegative plasma to an electropositive edge plasma. Since the two species electropositive plasma is well characterized, this matching is straightforward. The

edge region has the usual profile expressed in terms of sinusoids. A simple analytical solution to the two-region problem can be obtained by expanding the sinusoids to quadratic order. This does not give the correct edge profile, but allows a reasonably accurate calculation of the plasma parameters in the electronegative central plasma region. The main limitation of the theory is the tendency for low pressure capacitively coupled r.f. discharges to develop non-Maxwellian temperature distributions. In particular, efficient sheath heating tends to develop higher temperature tails to the distribution which effectively control the ionization rate. These distributions have been observed experimentally, and in both electropositive and electronegative plasma simulations [8,19]. They have been shown to significantly affect the self-consistent equilibrium of electropositive plasmas, while not being readily amenable to a self-consistent analytical determination [8]. We have found a similar situation to hold for electronegative plasmas, and have used the ratios of the temperatures and densities for the hot tail and the cooler bulk distributions, found in simulation, as input parameters for our analytic modeling.

As can be seen from the electron energy distribution functions in Fig. 3, the assumption of a two-temperature Maxwellian is somewhat arbitrary. In fact, the high temperature tails of the distribution fit better to a power law in energy, appropriately truncated at low energies. Power law distributions also have some justification from the theory of sheath heating [20] and increase the value of electron density, obtained from energy balance, in an electropositive plasma, giving better agreement

with simulation [8]. However, the assumption of a power law removes the simplicity of the exponential factors in the reaction rates, and also the use of the Boltzmann factors in the basic equations.

Rather than attempt such a basic overhaul of the theory, we re-examine the high pressure case in which a third, higher temperature tail to the distribution is employed. From Fig. 3 we estimate a higher temperature tail is a factor of 2 higher than the intermediate temperature with a density a factor of 26 below that of the main distribution. Using $\alpha_0 = 11.1$ and $\ell/\ell_p = 0.69$, from the previous calculation, which are not expected to change much, the new electron temperatures are calculated from (3.14), in which the two hotter distributions are used on the left hand side, and the ionization from the warm bulk is neglected. The result gives $T_{eh} = 5.6$ eV and $T_{ew} = 2.8$ eV. Recalculating α_0 from (3.15) but now neglecting both hot distributions, we obtain $\alpha_0 = 10.5$, a small improvement over the previous result, when compared to the simulation. We conclude that small improvements in the equilibrium can be obtained by improving the approximation to the electron energy distribution function, but these improvements are not essential.

Finally, it is clear that for a fully self-consistent analytic model, a method for calculating the density and temperature ratios for the two electron distributions will need to be devised. This is equally true for electropositive and electronegative plasmas. At higher neutral pressures, or in other types of discharges in which ohmic dissipation is the dominant heating mechanism, a single temperature Maxwellian

is a good approximation to the electron energy distribution function. In these situations, the analytic model developed here should adequately describe the plasma equilibrium.

Acknowledgement

The authors wish to acknowledge the support of the Department of Energy under DOE Grant DE-FG03-87ER13727 and Livermore U.S. Department of Energy Contract W-7405-ENG-48.

References

1. G. R. Missium, A. J. Lichtenberg, and M. A. Lieberman, *J. Vac. Sci. and Tech.*, **A7**, 1007 (1989).
2. J. H. Keller and W. P. Penebaker, *IBM Res. Div.*, **23**, 3 (1979).
3. J. A. Tailet, *J. Phys. Lett.*, **40**, 223 (1979) (Paris).
4. V. A. Godyak, *Soviet Radio Frequency Discharge Research*, Delphic Assoc. Inc., Falls Church, VA (1986).
5. M. A. Lieberman, *IEEE Trans. on Plasma Sci.*, **16**, 638 (1988).
6. D. Vender and R. Boswell, *IEEE Trans. on Plasma Sci.*, **18**, 725 (1990).
7. M. Surendra and D. B. Graves, *IEEE Trans. on Plasma Sci.*, **19**, 144 (1991).
8. B. Wood, "Sheath Heating in Low Pressure Capacitive R.F. Discharges," Thesis, University of California, Berkeley (1991).
9. J. B. Thompson, Research Notes, *Proc. Royal Soc.*, **73**, 818 (1959).
10. R. L. F. Boyd and J. B. Thompson, *Proc. Royal Soc.*, **A252**, 102 (1959).
11. H. Ameniya, *J. Phys. Soc. Jap.*, **57**, 887 (1988).
12. K.-U. Riemann, *J. Phys. D: Appl. Phys.*, **24**, 493 (1991).
13. R. W. Boswell, A. J. Lichtenberg, and D. Vender, *IEEE Trans. on Plasma Sci.*, **20**, 62 (1992).
14. P. D. Edgley and A. Von Engel, *Proc. Roy. Soc.*, **A370**, 375 (1980) (London).
15. F. A. Haas, L. M. Lea, and A. J. T. Holmes, *J. Phys. D: Appl. Phys.*, **24**, 1541 (1991).
16. e.g. see E. A. Mason and E. W. McDaniel, *Transport Properties of Ions in Gases*, John Wiley (1988); A. V. Phelps, JILA Information Center Report 28, University of Colorado, Boulder (1985).
17. V. Vahedi, "Modeling and Simulation of R.F. Discharges Used for Plasma Processing," Ph.D Dissertation, University of California, Berkeley (1993).
18. G. L. Rogoff, *J. Phys. D: Appl. Phys.*, **18**, 1533 (1985).
19. V. Vahedi, M. A. Lieberman, C. K. Birdsall, T. D. Rognlien, J. R. Hiskes, and R. H. Cohen, 45th Annual Gas. Elec. Conf., LA-11, Boston (1992).
20. C. G. Goedde, A. J. Lichtenberg, and M. A. Lieberman, *J. Appl. Phys.*, **64**, 4375 (1988).

Figure Captions

Fig. 1 Comparison of the density profiles of the simulation with the numerical solution of (2.16); n_{e0} and $\alpha_0 = n_{-0}/n_{e0}$ are matched to the simulation values in the numerical solution.

Fig. 2 Comparison of the density profile of n_- of the simulation with the parabolic analytical approximation (3.2).

Fig. 3 Two-temperature electron energy distributions obtained for (a) $p = 50$ mTorr neutral pressure, lower density plasma; and (b) $p = 10$ mTorr neutral pressure, higher density plasma.

Fig. 4 Comparison of analytic solution with simulation; n_{e0} and $\ell_p(u_i = u_B)$ for the analytic solution are matched to the simulation results; $p = 50$ mTorr (large α) case.

Fig. 5 Comparison of analytic solution with simulation; n_{e0} and α_0 are matched; $p = 10$ mTorr (small α) case.

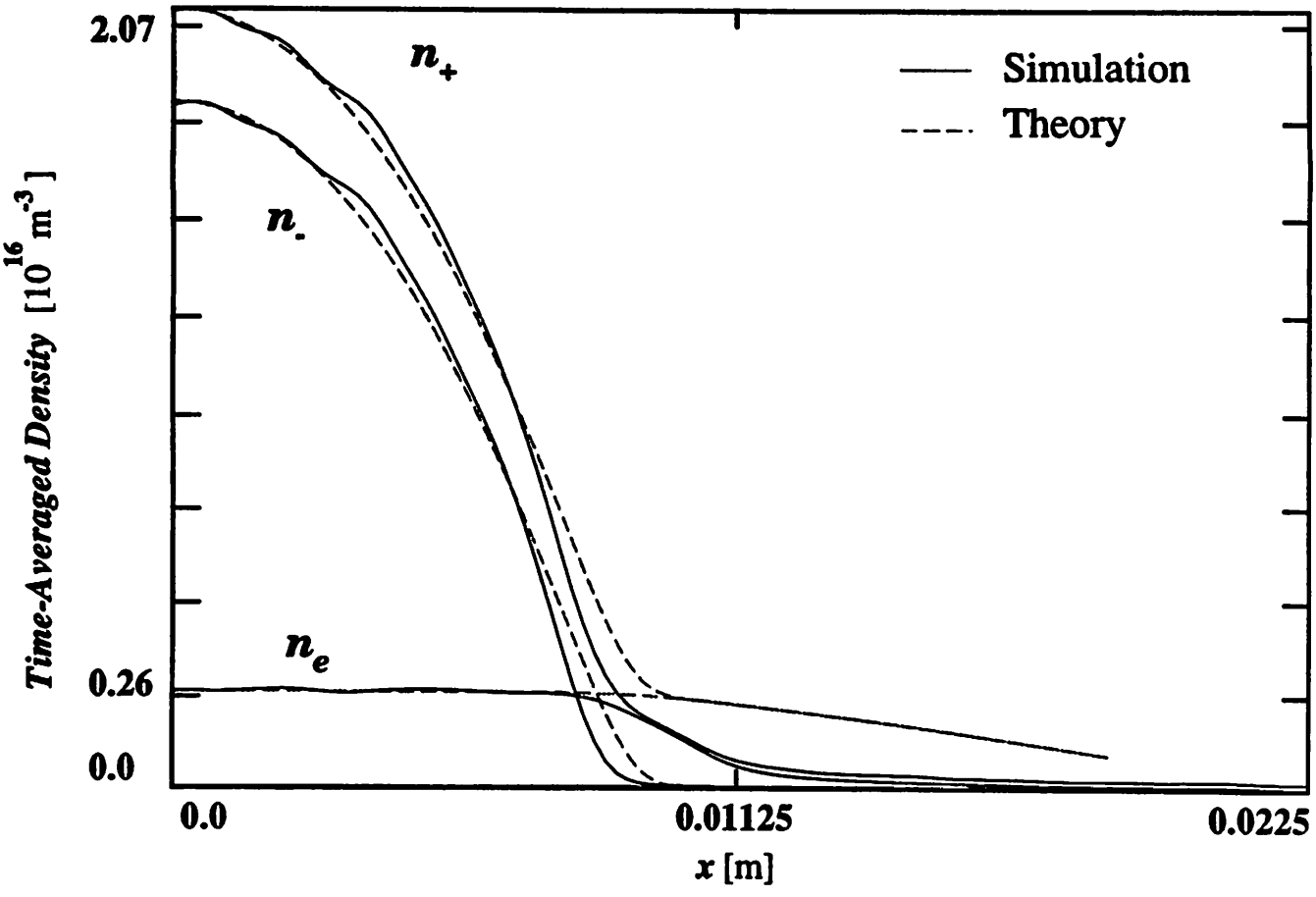
2.07
0.26
0.0
n_+
n_-
n_e
Simulation
Theory
Time-Averaged Density [10^{16} m^{-3}]
0.0
0.01125
0.0225
x [m]

Figure 1

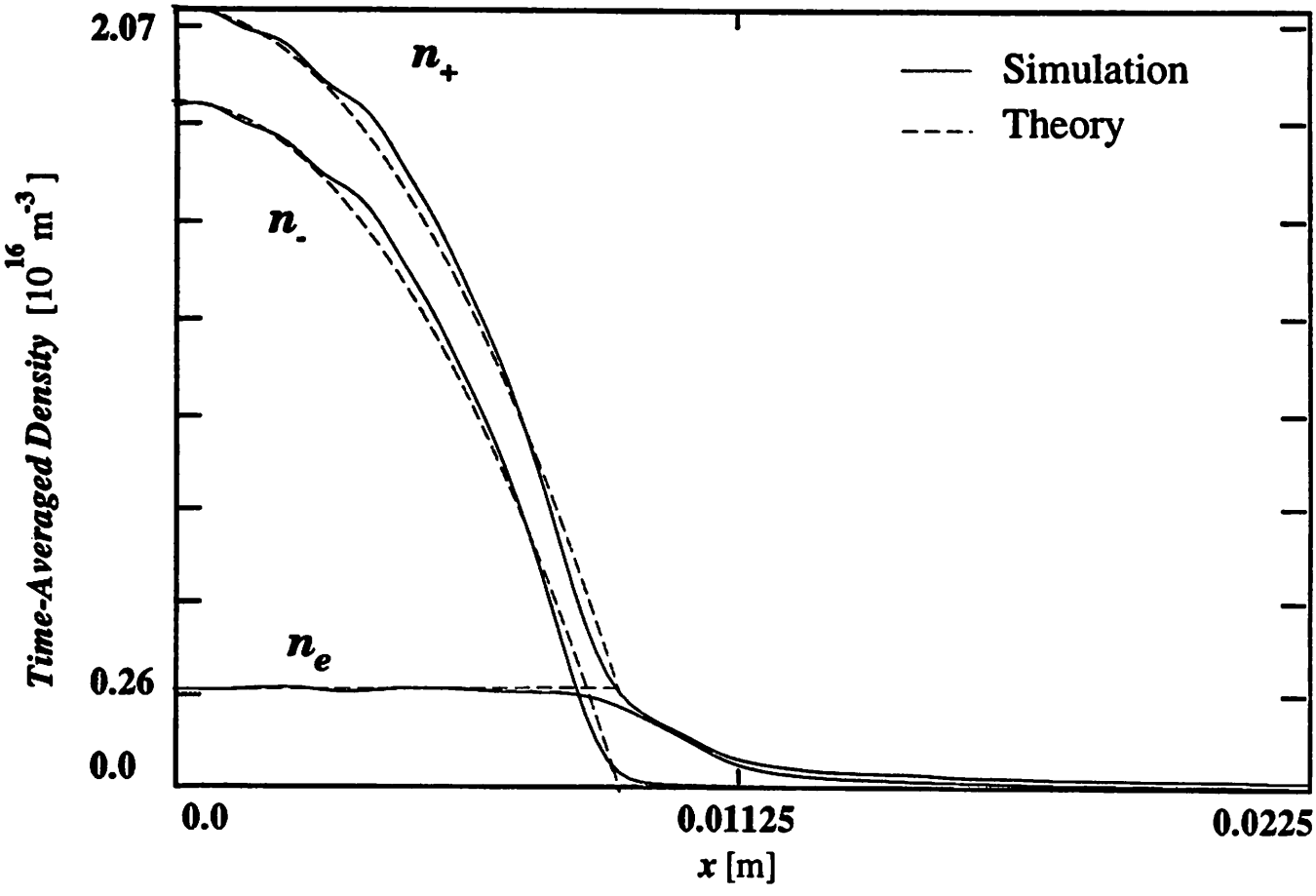
2.07
0.26
0.0
n_+
n_-
n_e
Simulation
Theory
Time-Averaged Density [10^{16} m^{-3}]
0.0
0.01125
0.0225
x [m]

Figure 2

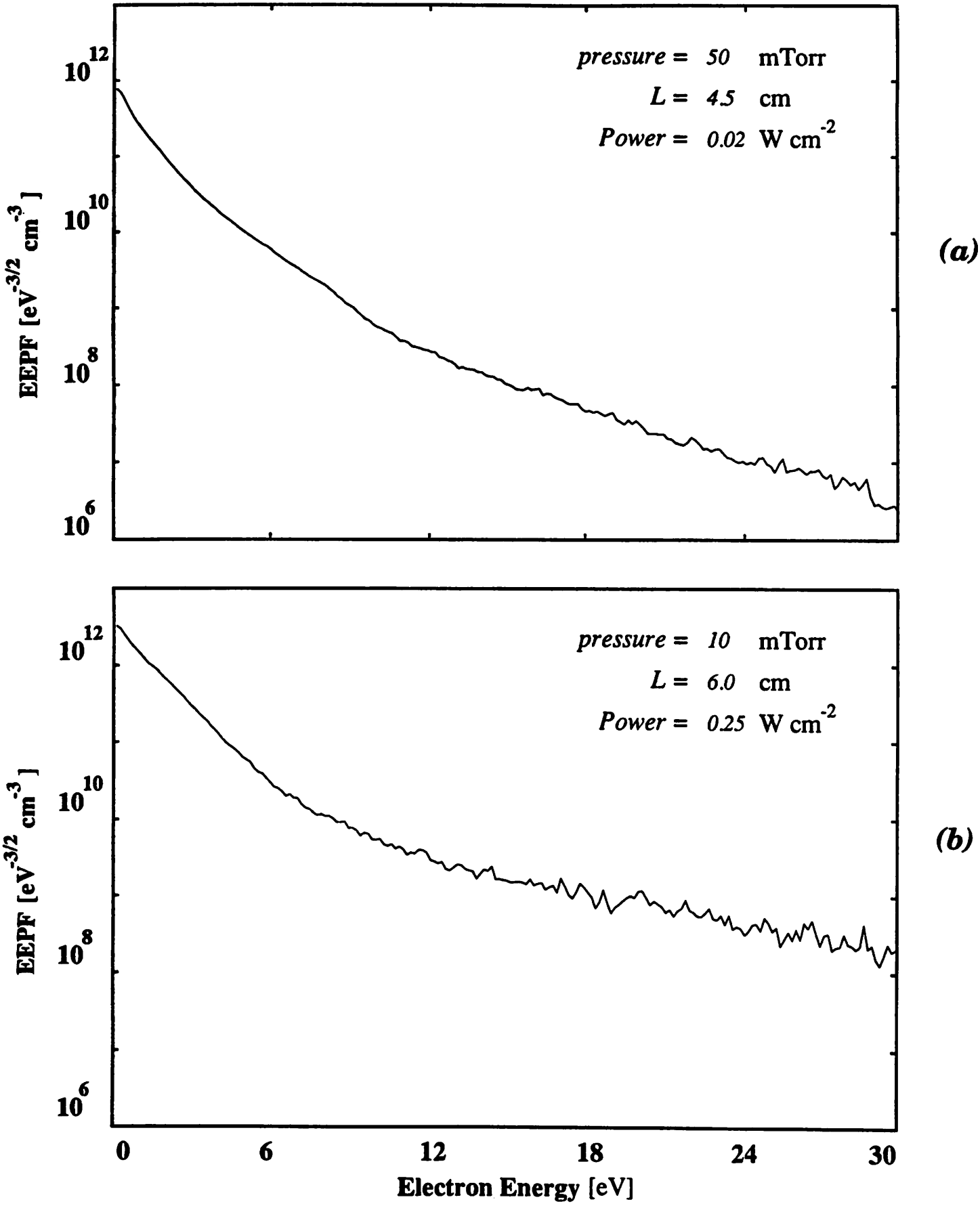
pressure = 50 mTorr
L = 4.5 cm
Power = 0.02 W cm-2
EEPF [eV-3/2 cm-3]
10^12
10^10
10^8
10^6
(a)
pressure = 10 mTorr
L = 6.0 cm
Power = 0.25 W cm-2
EEPF [eV-3/2 cm-3]
10^12
10^10
10^8
10^6
(b)
0
6
12
18
24
30
Electron Energy [eV]

Figure 3

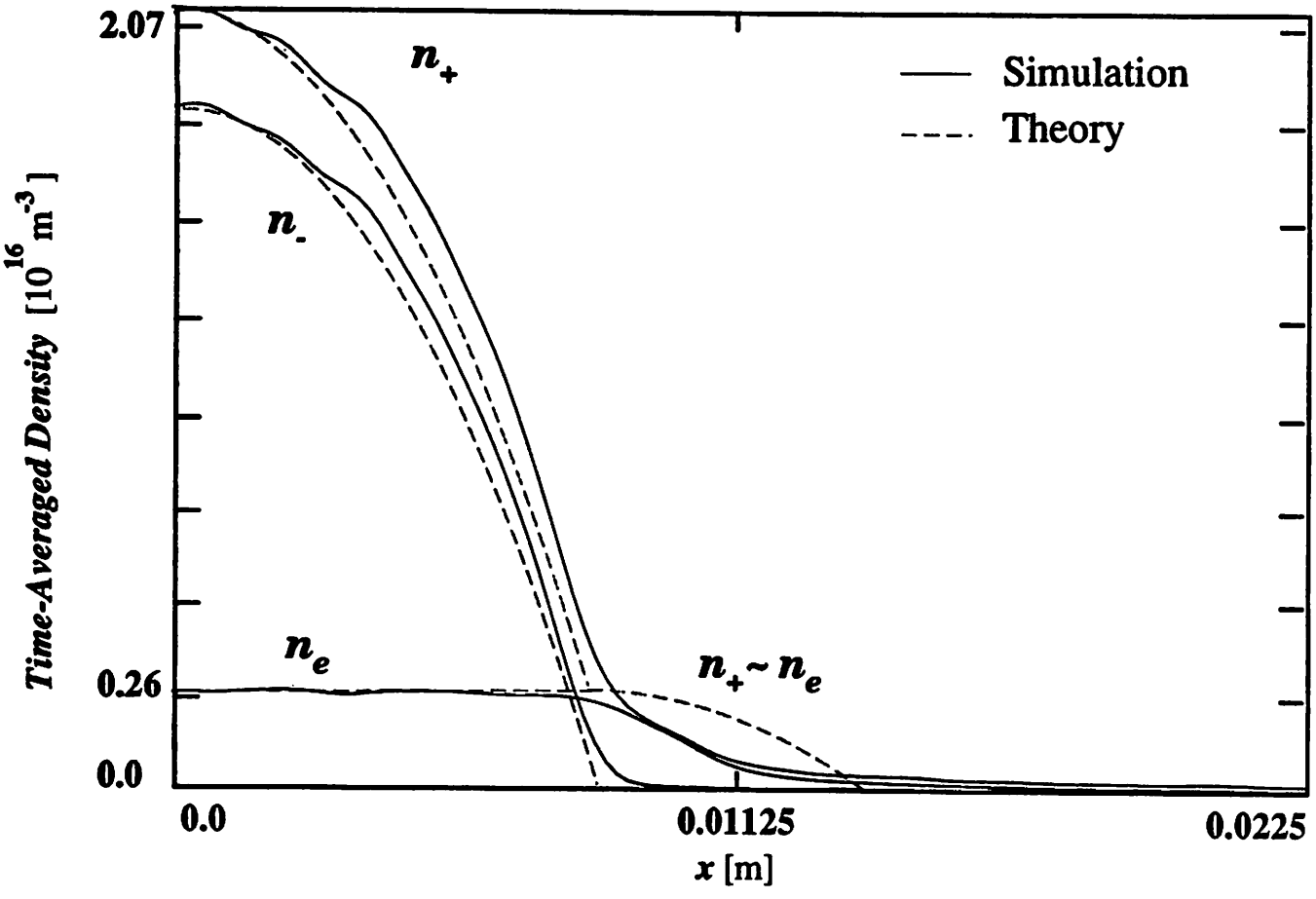
2.07
0.26
0.0
n_+
n_-
n_e
$n_+ \sim n_e$
Simulation
Theory
Time-Averaged Density [10^{16} m^{-3}]
0.0
0.01125
0.0225
x [m]

Figure 4

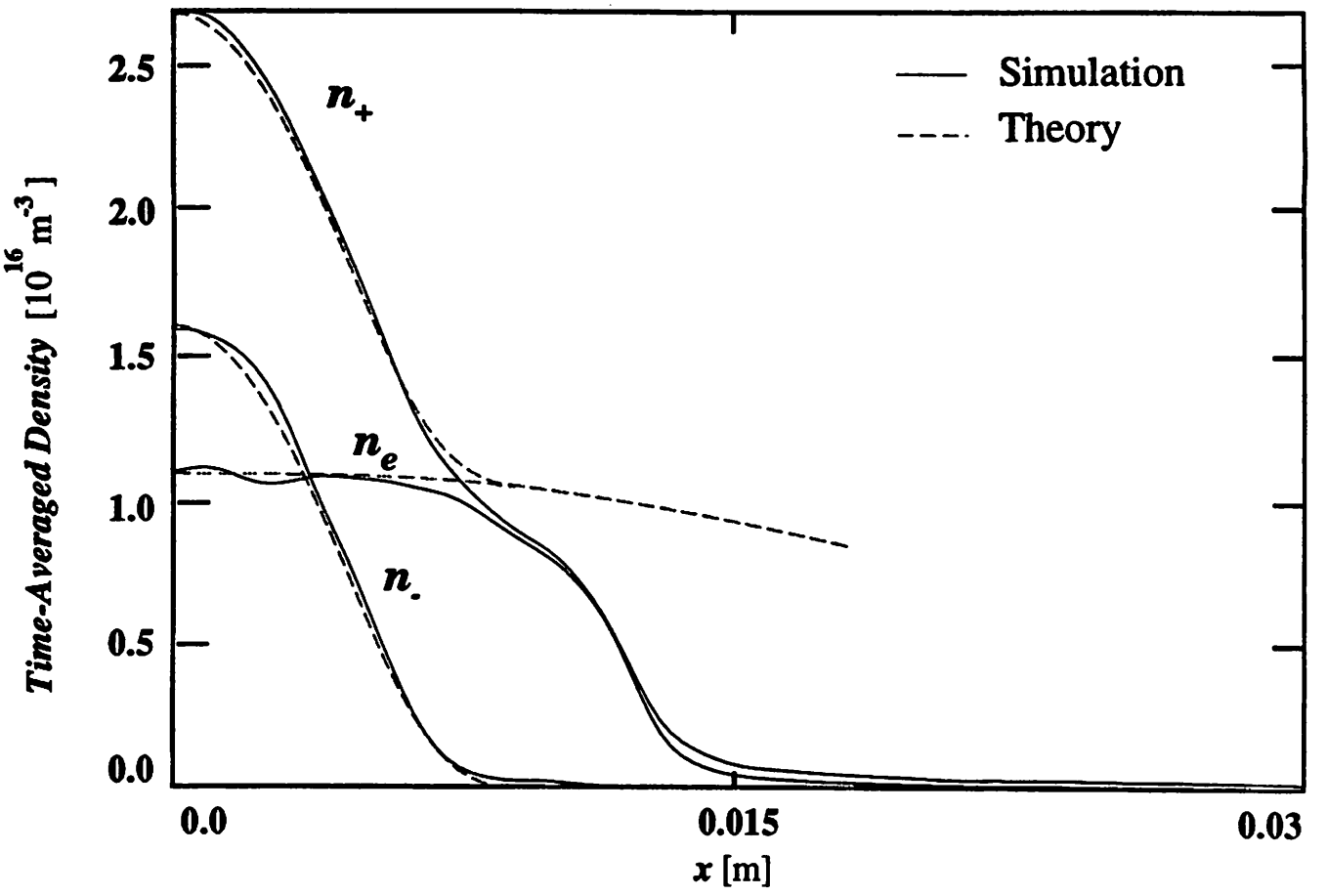
Simulation
Theory
n_+
n_e
n_-
2.5
2.0
1.5
1.0
0.5
0.0
0.0
0.015
0.03
x [m]
Time-Averaged Density [10^{16} m^{-3}]

Figure 5

ERRATA

Modeling Electronegative Plasma Discharges

by

A. J. Lichtenberg, V. Vahedi, M. A. Lieberman, and T. Rognlien

pg 4, middle: "rule" should read "rate"

pg 5, Eq (2.1):

$$\Gamma_i = -D_i \nabla n_i \pm n_i \mu_i E_i$$

pg 11, 1st para: "following section" should read "section IV"

pg 12, Eq (3.1):

$$-2D_+ \frac{d^2 n_+}{dx^2} = K_{iz} n_0 n_{e0},$$

pg 15, Eq (3.14):

$$P_{abs} = -2\mathcal{E}_c D_{a+} \frac{dn_+}{dx}\bigg|_{x=\ell_p} + 2\mathcal{E}_c \int_0^{\ell} K_{rec} n_+ n_- dx.$$

pg 15, below Eq (3.14): $n_{-0} \simeq n_{+0}$

pg 17, below Eq (3.17): (3.15) should read (3.16)

pg 20, 2nd & 3rd para: (3.14) should read (3.15)

pg 21, last para: (4.1) should read (4.2)

pg 22, 2nd para: (4.9b) should read (4.1b)

(3.14) should read (3.15)